JOURNAL OF GEOPHYSICAL RESEARCH: OCEANS, VOL. 118, 847–855, doi:10.1029/2012JC008354, 2013

Atlantic water variability on the SE Greenland continental shelf and its relationship to SST and bathymetry

David A. Sutherland,[1] Fiammetta Straneo,[2] Garry B. Stenson,[3] Fraser J.M. Davidson,[3] Mike O. Hammill,[4] and Aqqalu Rosing-Asvid[5]

Received 11 July 2012; revised 5 December 2012; accepted 6 December 2012; published 20 February 2013.

[1] Interaction of warm, Atlantic-origin water (AW) and colder, polar origin water (PW) advecting southward in the East Greenland Current (EGC) influences the heat content of water entering Greenland's outlet glacial fjords. Here we use depth and temperature data derived from deep-diving seals to map out water mass variability across the continental shelf and to augment existing bathymetric products. We compare depths derived from the seal dives with the IBCAO Version 3 bathymetric database over the shelf and find differences up to 300 m near several large submarine canyons. In the vertical temperature structure, we find two dominant modes: a cold mode, with the typical AW/PW layering observed in the EGC, and a warm mode, where AW is present throughout the water column. The prevalence of these modes varies seasonally and spatially across the continental shelf, implying distinct AW pathways. In addition, we find that satellite sea surface temperatures (SST) correlate significantly with temperatures in the upper 50 m ($R = 0.54$), but this correlation decreases with depth ($R = 0.22$ at 200 m), and becomes insignificant below 250 m. Thus, care must be taken in using SST as a proxy for heat content, as AW mainly resides in these deeper layers. Sample Unit Level Copyright

Citation: Sutherland, D. A., F. Straneo, G. B. Stenson, F. J. M. Davidson, M. O. Hammill, and A. Rosing-Asvid (2013), Atlantic water variability on the SE Greenland continental shelf and its relationship to SST and bathymetry, *J. Geophys. Res. Oceans*, *118*, 847–855, doi:10.1029/2012JC008354.

1. Introduction

[2] The Greenland ice sheet underwent rapid and large changes over the decade 2000-2010 [*Zwally et al.*, 2011; *Rignot et al.*, 2011], with increased net mass loss observed via many of its outlet glaciers [*Howat et al.*, 2007; *Stearns and Hamilton*, 2007]. Glaciers in southeast Greenland, in particular, accelerated in the early 2000s and peaked in 2005, while glaciers in west Greenland showed mixed velocity variability [*McFadden et al.*, 2011]. Causes for these dynamic changes are still not well understood, but hypotheses usually include a combination of increased surface melting that drives more lubricating meltwater to the glacier bed, with a) increased submarine melting, and/or b) loss of the buttressing ice mélange due to changes in ocean heat transport [*Vieli and Nick*, 2011]. The ocean regulation hypothesis has received attention recently in studies showing complex and highly variable fjord circulation in Greenland's outlet glacial fjords [*Holland et al.*, 2008; *Straneo et al.*, 2010; *Murray et al.*, 2010; *Rignot et al.*, 2010].

[3] Despite an emphasis on obtaining ocean measurements around Greenland, the observational record on the continental shelf is scarce in space and time. South of Denmark Strait, warm waters from the Irminger Sea flow southward in the Irminger Current (IC) alongside the cold Arctic waters that advect southward in the East Greenland Current (EGC) [*Rudels et al.*, 2002; *Dodd et al.*, 2009]. A sharp temperature and salinity front separates the IC and EGC in the horizontal and is usually located over the shelfbreak and continental slope [e.g., *Sutherland and Pickart*, 2008]. However, the slope waters from the Irminger Sea also penetrate into the submarine canyons that cut into the SE Greenland continental shelf, so a vertical layering of water masses occurs, with warmer Irminger Sea water overlain by colder EGC waters [*Rudels et al.* 2002; *Dodd et al.*, 2009]. Hydrography from glacial fjords around Greenland all exhibit this cold/warm layering to some extent, with the temperature of the warm, salty Atlantic-origin water dependent on the distance from a source [*Straneo et al.*, 2012]. For example, in SE Greenland, the Atlantic-origin waters (AW) derive mainly from the Irminger Sea—hereafter we use AW and Irminger Sea waters interchangeably, though we note this holds true only for Sermilik Fjord, as Kangerdlugssuaq Fjord may be influenced by multiple AW sources (see below).

[4] Inside Sermilik Fjord, the two-layer stratification generally results in a 150 m thick polar water (PW) layer inherited

All Supporting Information may be found in the online version of this article.

[1]Department of Geological Sciences, University of Oregon, Eugene, Oregon, USA.
[2]Department of Physical Oceanography, Woods Hole Oceanographic Institution, Woods Hole, Massachusetts, USA.
[3]Department of Fisheries and Oceans, St. John's, Newfoundland, Canada.
[4]Department of Fisheries and Oceans, Mont-Joli, Quebec, Canada.
[5]Department of Birds and Mammals, Greenland Institute of Natural Resources, Nuuk, Greenland.

Corresponding author: D. A. Sutherland, Department of Geological Sciences, 1272 University of Oregon, Eugene, Oregon 97403-1272, USA. (dsuth@uoregon.edu)

2169-9275/13/10.1029/2012JC008354

from the EGC waters, residing above the warmer AW [*Straneo et al*., 2010]. The fact that the deep AW layer derives from the Irminger Sea implies that some slope current or interior water makes it into the fjord, albeit in a modified, colder form. However, the pathways and transformation of AW on the continental shelf are still poorly understood due to a lack of measurements and accurate bathymetry, challenging current ocean general circulation and climate models including those attempting to resolve ice sheet-ocean interactions [e.g., *Jin et al*., 2011]. Furthermore, several studies have used satellite-derived sea surface temperature (SST) as a proxy for AW variability on the continental shelf and in the fjords [*Murray et al*., 2010; *Hanna et al*., 2009]; it is unclear, however, how changes in the properties of the AW in the fjords are related to SST since both in the fjords and on the shelf AW is typically found beneath PW.

[5] In the Southern Ocean, several recent studies have begun to analyze oceanographic processes from instrumented marine mammals to map out pathways of water infiltrating under Antarctica's ice shelves, as well as constraining available bathymetric products [e.g., *Nicholls et al*., 2008; *Padman et al*., 2012]. Here we describe a new dataset over the SE Greenland shelf consisting of remotely sensed marine mammal tag information that includes temperature, depth and location. The data presented here have been used previously to examine the migratory behavior of the hooded seal (*Cystophora cristata*) [*Andersen et al*., 2009], and as part of a 1° x 1° temperature climatology of the North-West Atlantic Ocean [*Grist et al*., 2011]. The latter study stressed the importance of boundary currents along the Greenland coast, but lacked the resolution to analyze features on the continental shelf.

2. Seal Data

[6] Between 2004 and 2010, a total of 104 individual seals were fitted with satellite relay depth loggers (SRDLs) that reported time, maximum dive depth, and location. We used SRDL Series 9000 units manufactured by the Sea Mammal Research Unit of St. Andrews University, UK [e.g., *Lydersen et al*., 2004; *Boehme et al*., 2009]. Raw location data are determined by the Argos satellite system and subsequently filtered using an algorithm based on the speed of the animal between location fixes [*Freitas et al*., 2008]. The SRDLs are also equipped with temperature sensors (0.1 °C resolution) that sample at one second intervals on the ascent. To preserve battery power, these full-resolution data are subsampled using the "broken-stick" compression algorithm [*Kerr*, 1984] that is also used for data reduction in XBT casts [*Rual*, 1996]. For these SRDLs, this data reduction results in 12 temperature-depth values picked to reproduce the actual temperature structure of each dive [*Fedak et al*., 2002]. A comparison of temperature profiles derived from similar SRDLs with full resolution conductivity-temperature-depth (CTD) profiles in the Southern Ocean showed good agreement for temperature values [*Roquet et al*., 2011].

[7] Only 56 of these individuals moved through the SE Greenland region on their annual migration (Figure 1). The majority were hooded seals (54 individuals), with only 2 harp seals (*Phoca groenlandica*). In total, there were 37011 dives in SE Greenland, with 4339 inside the Sermilik Fjord sub-region (box SF), and 3704 and 2997 dives in the Cape Farewell (box CF) and Kangerdlugssuaq regions (box KG), respectively (Figure S1). Tagging locations

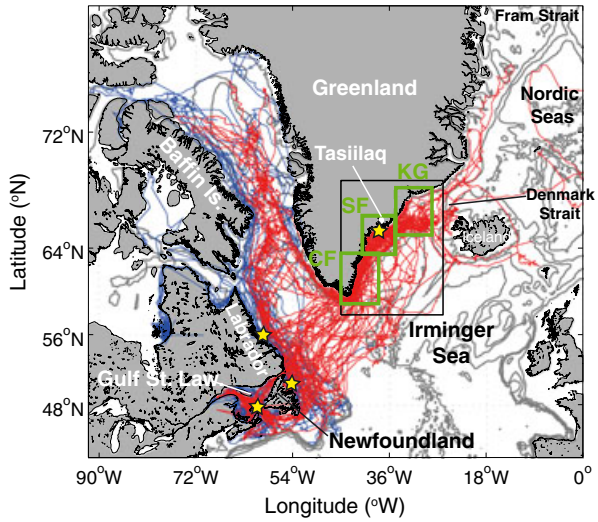

Figure 1. Regional map showing place names and the location of all seal tracks originating from Canada and Greenland (stars). Tracks passing inside (red) or outside (blue) the SE Greenland region (black) were subdivided into continental shelf regions (green boxes) near Sermilik Fjord (SF), Cape Farewell (CF) and Kangerdlugssuaq Fjord (KG). GEBCO bathymetry is contoured at 200, 1000, 2000, and 3000 m.

varied in space and time (Figure 1; Table 1). Hooded seals fitted with a SRDL in summer were captured post-moult in SE Greenland (Figure 1). The remaining hooded seals were located and tagged in spring breeding grounds off Canada [*Andersen et al*., 2009]. The harp seals were tagged in June off Newfoundland, following their annual moult. Hooded seals feed primarily on benthopelagic species and can dive in excess of 1500 m, suggesting that they can easily reach the seabed [*Hammill and Stenson*, 2000; *Rosing-Asvid*, 2010]. Harp seals are more shallow divers with the majority of dives being less than 100 m [*Stenson*, unpublished data].

3. Seal-Derived Temperatures

3.1. Summertime Mean Temperature Fields

[8] We first use the seal-derived temperature (T) data to construct mean T fields based on dives during the summer season (JJA) when there are sufficient numbers to get a dequate horizontal coverage (Figure S1). Each seal dive results in a vertical temperature profile, $T(z)$, with 12 temperature-depth pairs. We interpolate $T(z)$ onto a regular vertical grid with 5-m spacing. Next we bin the profiles into non-overlapping 5 km x 5 km regions and average all the profiles in each box over 50-m thick depth layers (e.g., T_{0-50} corresponds to the 0–50 m layer average). We averaged over 50-m thick vertical layers in order to control the total number of layers analyzed, while keeping the layer thickness small enough to retain resolution in the vertical and capture the typical stratification present in this region. Results using 20-m thick layers were not significantly different, while using 100-m thick layers would alias the results as the PW layer can be shallower than 100-m at certain times. The horizontal bin size of 5 km was chosen to balance the desire for high-resolution T fields (on the order of the deformation radius) with having enough dives per bin to obtain significant results. Temperatures in box/layer combinations with zero or one seal dive were omitted,

Table 1. Summary of Seal Tagging Information for 2004-2010 for Seals That Crossed into the SE Greenland Shelf Region, see Figure 1[a]

Year	# Seals	Species	Location[b]	Month[c]	Duration[d] (days)
2004	11	hooded	Newfoundland	March	95
	2	harp	Newfoundland	June	127
	1	hooded	SE Greenland	July	132
2005	5	hooded	Gulf of St. Lawrence	March	88
	7	hooded	SE Greenland	July	190
2006	4	hooded	Labrador	February	103
	7	hooded	Newfoundland	March/April	72
2007	4	hooded	SE Greenland	July	170
2008	5	hooded	Gulf of St. Lawrence	March	94
	7	hooded	Newfoundland		81
2010	3	hooded	Newfoundland	March	112

[a]See *Andersen et al.* [2009] and *Grist et al.* [2011] for more information on these seal tracks and dives.
[b]Time of year that seals were tagged, see text for details.
[c]Average duration of these tags in days.
[d]General location of where the seals were tagged (Figure 1).

resulting in T fields as illustrated in Figure 2. The coverage of seal dives that went into these distributions (see example in Figure 3d) varied across the continental shelf, giving a range of standard errors ($\sigma / N^{1/2}$) from 0–5.6 °C for $T_{0–50}$ in the SF sub-region (Figure 3c).

[9] The mean summertime temperature fields illustrate the importance of bathymetry in channeling flows along the SE Greenland coast. Warm ($T > 6$ °C), Irminger Sea water is found seaward of the continental shelf/slope region at all depths (Figure 2). The coldest water, stemming from the polar-origin EGC, is found at shallow depths ($z < 150$ m) on the bank north of the submarine canyon extending towards Sermilik Fjord, then in a narrow band sandwiched between the coast and the warmer IC water. This is consistent with the observed behavior of the East Greenland Coastal Current (EGCC) in this area [*Bacon et al.*, 2002; *Sutherland and Pickart*, 2008]. The warm water intrudes along the 300-400 m isobath in all layers, creating strong horizontal temperature gradients in the upper 150 m. Downstream of Sermilik Fjord, colder water is found again in a widened band, suggesting the intrusion of AW is a meander of the IC along with the EGC towards the coast. Another possibility is that anticyclonic eddies spun off the IC propagate shoreward, carrying their warm and salty anomalies relatively intact.

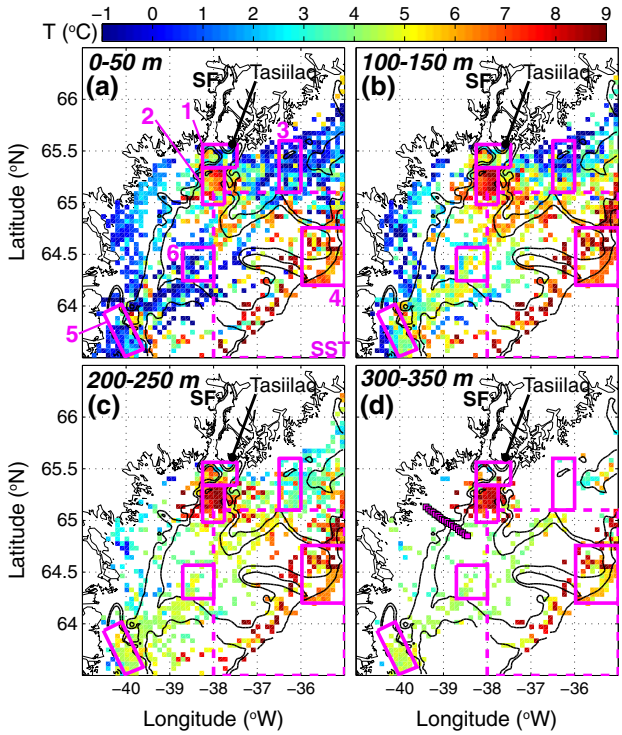

Figure 2. (a) The seal-derived summertime $T_{0–50}$ field for the Sermilik Fjord (SF) region. Updated bathymetry (GEBCO plus seals) is shown for the 300- and 400-m isobaths. Boxed regions show areas where AW variability was analyzed (solid magenta, 1-6; see Table 2) and SST correlations were made (dashed magenta). (b) Same as a, but for $T_{100–150}$. (c) Same as a, but for $T_{200–250}$. (d) Same as a, but for $T_{300–350}$. The August 2004 CTD stations are marked (magenta squares).

[10] The Kangerdlugssuaq Fjord and Cape Farewell sub-regions (Figure S2 and S3, respectively) display similar patterns for $T_{0–50}$, with warmer water primarily offshore of the continental shelf-slope region, except near bathymetric irregularities, where the warmer water turns shoreward. The Kangerdlugssuaq Trough (Figure S2) significantly influences $T(z)$ there [*Murray et al.*, 2010]. Upstream of the trough, the $T(z)$ fields above 150 m suggests that AW from the Irminger Sea veers onto the shelf, consistent with conservation of potential vorticity as the EGC feels the deep trough downstream. In the deeper layers, however, colder water is present east of the trough, which might indicate the presence of a different Atlantic-origin water mass such as return Atlantic water (RAW) that has been modified and lost heat along its route through the Arctic Ocean and/or the Nordic Seas [*Rudels et al.*, 2002].

3.2. AW Variability and Vertical Temperature Structure

[11] To investigate the different potential pathways of AW and their variability in time, we examine the un-averaged T profiles inside the Sermilik Fjord sub-region. First, we define six regions based on the summertime $T_{0–50}$ fields and underlying bathymetry (Table 2; Figure 2a) and group the dives in each region together. The regions were chosen to capture different temperature variability based on the fields shown in Figure 2 and from previous circulation schematics

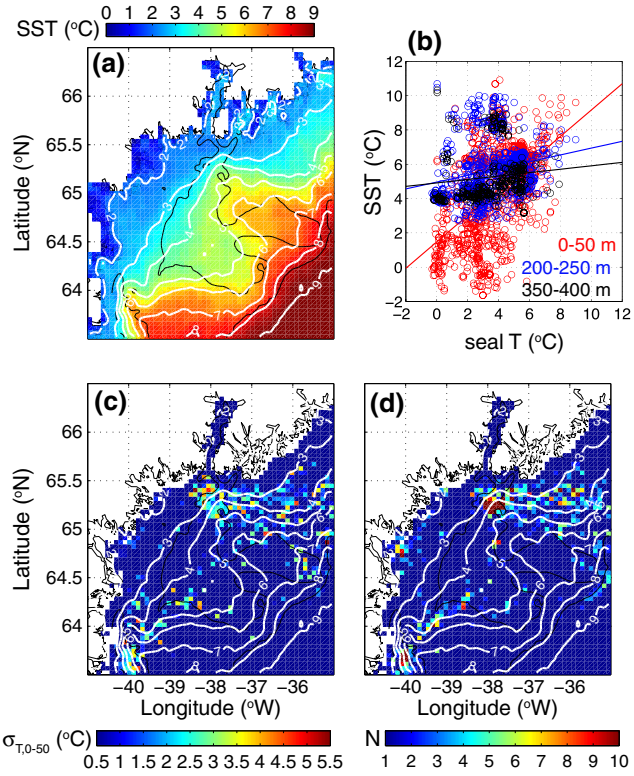

Figure 3. (a) 2004–2010 mean SST over summer from the monthly 9 km MODIS SST product. The 400-m bathymetric contour (GEBCO plus seal) is shown (black) along with select SST isotherms (white). (b) Correlations between interpolated SST with seal $T_{a,0\text{-}50}$ (red), $T_{a,200\text{-}250}$ (blue), and $T_{a,350\text{-}400}$ (black) along with best-fit lines. (c) Standard deviation, σ, of $T_{0\text{-}50}$ with isotherms from a overlaid. Gaps in seal coverage were set to 0 to ease comparison. (d) Same as c but for number of dives, *N*, per bin.

Table 2. Characteristics of Boxed Regions in the Sermilik Fjord (SF) Subregion (Figure 2a)

Box	General area	Total # of profiles	% warm mode
1	Outside SF mouth	841	29%
2	In canyon leading to SF mouth	134	19%
3	Shallow bank; upstream of SF	184	12%
4	Irminger Sea; Shelfbreak	186	78%
5	In separate canyon south of SF	163	17%
6	In canyon downstream of SF	87	10%

[e.g., *Sutherland and Pickart*, 2008]. Care was taken to group profiles in areas of uniform depth and to capture the important end-members. For example, box 4 covers the Irminger Sea, while box 3 is on the shallow upstream shelf.

[12] The resulting *T* profiles (Figure 4) share several characteristics: 1) deeper waters (>150 m) are typically warm (>4 °C) with little variation over the bottom part of the water column, 2) waters above 150 m alternate between being relatively cold or at a similar *T* to deeper waters, and 3) *T* in the surface layer (<50 m) are widely variable, suggesting that seasonal air-sea fluxes or sea ice melt significantly alters temperatures there.

[13] The *T* profiles fall into 2 main groups, depending on the degree of vertical *T* stratification (Figure 4). To quantify this, we calculate a *T* difference (ΔT) between 200 m and 50 m (to avoid the surface variability), for all profiles >200 m deep. A large ΔT ($\Delta T > 0.5$ °C) indicates profiles resembling properties typically observed in the EGC and inside Sermilik Fjord [*Rudels et al.*, 2002; *Straneo et al.*, 2010]. We call this mode the "cold" mode, as PW are present in the upper water column. In contrast, the second dominant mode ($\Delta T < 0.5$ °C), are relatively warm profiles with no vertical variation, indicating the presence of AW throughout the water column. We call this mode the "warm" mode, as PW are absent.

[14] We hypothesize that the warm mode profiles must derive from the interior of the Irminger Sea, outside the influence of the EGC where temperature values match those found in the warm mode profiles. To test this, we looked at the prevalence of the two modes in each region (Figure 4). A large majority (78%) of all profiles in box 4, located offshore of the EGC in the Irminger Sea, were warm mode, as expected (Table 2). In contrast, upstream of the fjord on the shallow ~300 m bank in box 3, the water is predominantly cold mode. However, IC eddies have been observed on the continental shelf and represent a source for the warm mode profiles there [*Sutherland and Pickart*, 2008; *Magaldi et al.*, 2011]. These IC eddies are anti-cyclonic, with a warm, salty core, and are distinct from the cyclones generated at the Denmark Strait overflow region [*Bruce*, 1995]. The relationship between these anticyclonic IC eddies and the overflow cyclones is unknown.

[15] The majority of all seal dives occurred in box 1, located near the mouth of Sermilik Fjord, but outside the channel where the EGC/EGCC is observed (Table 2). 29% of the box 1 profiles were warm mode, with some bottom $T > 8$ °C, suggesting that unmodified Irminger Sea water is advected this far inshore. There is no evidence that water this warm enters Sermilik Fjord, most likely due to bathymetric constraints and the EGC/EGCC acting as a barrier, forcing modification of the AW as it mixes with PW.

[16] Downstream of Sermilik Fjord, the *T* profiles from box 6 imply that the AW properties observed upstream in boxes 1 and 2 do not make it that far south, moving offshore again before entering this region. In another trough cutting towards the Greenland coast in box 5, the *T* structure resembles that from outside the mouth of Sermilik Fjord in box 1, but without the unmodified IC waters present. The absence of interior Irminger Sea water is presumably due to the lack of a pure advective AW pathway into this area, as well as being further alongstream in the EGC/IC system.

[17] The bimodal structure in the *T* profiles, interpreted here as variability in the pathway of AW onto the continental shelf, can also be traced seasonally. Figure 4g plots the percentage of seal profiles showing warm mode properties versus month for each box. Only month-box combinations with >10 seal profiles were included. Results did not change significantly when we used a cutoff of 5 seal profiles or 15 profiles. We chose to show month-box combinations with multiple seal profiles only to minimize spikes in the seasonal picture generated by having too few data points.

[18] The general trend is an increase in the prevalence of warm mode profiles over the summer and fall in box's 1, 2, and 6, with a coincident decrease in box 3. The limited data from offshore in box 4 shows no trend, with the warm mode dominating. Seasonally, observations of *T* on the continental shelf show a warming that starts during summer and

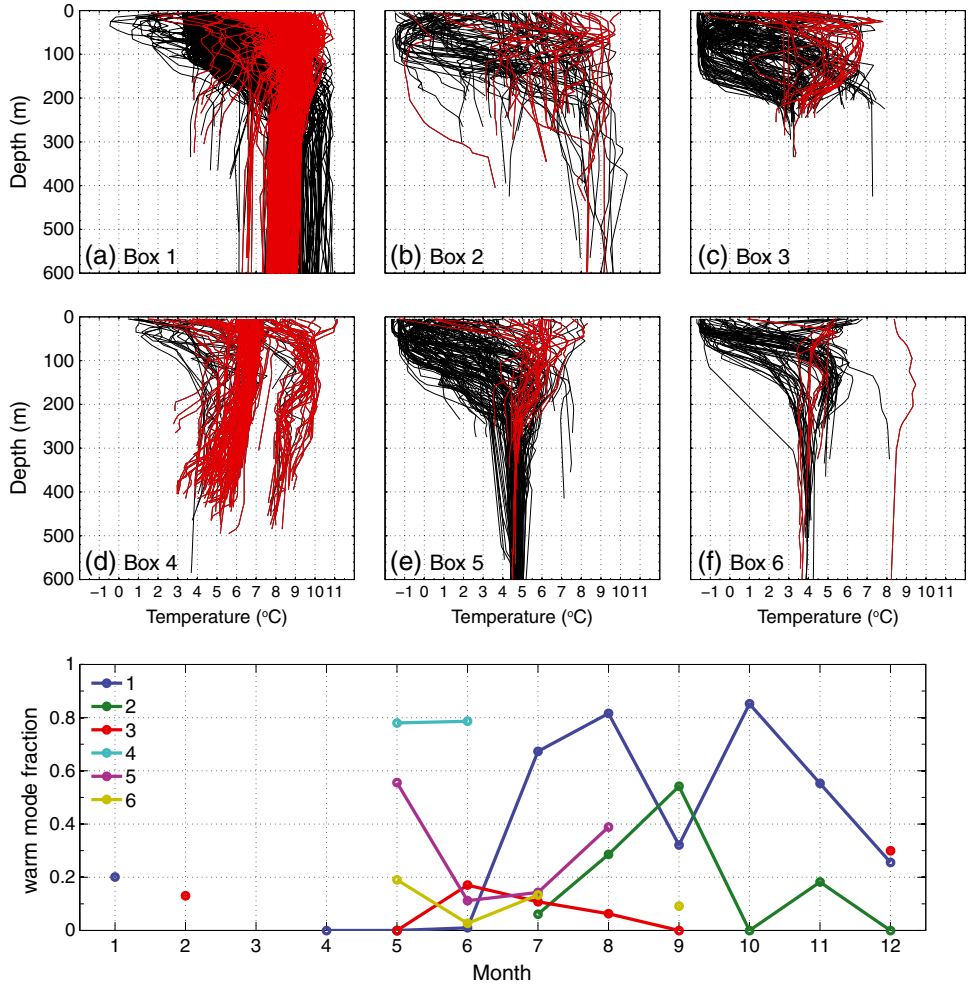

Figure 4. (a–f) Seal-derived temperature profiles vs. depth for each box in Figure 2. For profiles deeper than 200 m, color highlights "warm" mode (red) and "cold" mode (black), with the % of all warm mode profiles reported in Table 2. (g) Time series of the fraction of warm mode T profiles in each box as a function of month. Gaps indicate insufficient data for that month or box.

extends into fall [*Straneo et al.*, 2010], partly explaining the higher temperatures in box 1 versus box 4. However, this does not explain the AW variability, i.e., why the two modes are location dependent. We speculate that a reduction in the EGC during summer and fall would allow the IC to expand, increasing the prevalence of warm mode profiles observed outside Sermilik Fjord. The reduced strength in the EGC might also reduce the baroclinic instability mechanism responsible for the production of eddies along the shelfbreak, reducing the likelihood of IC eddies over the continental shelf upstream.

3.3. Correlations With SST

[19] We can also use the seal-derived T fields to investigate the utility of satellite SST data in characterizing subsurface ocean temperatures. To do this, we obtained monthly SST fields for the years 2004–2010 from the 9 km Level 3 MODIS Terra satellite data product [http://podaac.jpl.nasa.gov]. We then interpolated the SST data to the positions of each seal dive during the month they occurred, and compared them with the 50-m vertically averaged, but not horizontally binned, temperature profiles, $T_{a,0–50}$, $T_{a,50–100}$, etc. Monthly SST data were used since daily or 8-day products were frequently cloud-covered, which decreased the number of comparison points to a level too low for this analysis.

[20] Since MODIS SST data quality flags do not include the presence of sea ice, we restrict the analysis to a region away from the coast, where sea ice is rarely found even in winter, with the justification that a similar method would have to be used if utilizing SST as a proxy. Results from the analysis done over the entire region but for only the months of July to September (when sea ice is at a minimum), gave correlations slightly lower to those reported below, but did not change their significance or trend.

[21] Correlations between SST and $T_{a,0–50}$, as well as between all depths, are given in Table 3 and Figure 3b. We find a weak, but significant positive correlation of $R = 0.54$ ($p < 0.05$) between SST and $T_{a,0–50}$. The muted SST to $T_{a,0–50}$ correlation is likely due to the use of monthly data and the 50-m layer thickness. We find similar effects when comparing a temperature section (location in Figure 2d) from an August 2004 cruise [*Sutherland and Pickart*, 2008] with a section created from the seal temperatures averaged along the

Table 3. Correlations Between the Seal-Derived Temperature Profiles Averaged in 50-m Layers and Monthly SST Data[a]

	SST	$T_{a,0–50}$	$T_{a,50–100}$	$T_{a,100–150}$	$T_{a,150–200}$	$T_{a,200–250}$	$T_{a,250–300}$	$T_{a,300–350}$	$T_{a,350–400}$
$T_{a,0–50}$	**0.54**	--							
$T_{a,50–100}$	**0.31**	**0.84**	--						
$T_{a,100–150}$	**0.26**	**0.73**	**0.90**	--					
$T_{a,150–200}$	**0.25**	**0.70**	**0.80**	**0.94**	--				
$T_{a,200–250}$	**0.22**	**0.67**	**0.73**	**0.85**	**0.96**	--			
$T_{a,250–300}$	0.18	**0.69**	**0.77**	**0.87**	**0.94**	**0.98**	--		
$T_{a,300–350}$	0.15	**0.59**	**0.75**	**0.85**	**0.91**	**0.95**	**0.98**	--	
$T_{a,350–400}$	0.12	0.53	0.67	**0.79**	**0.86**	**0.91**	**0.94**	**0.98**	--
$T_{a,400–450}$	-0.01	0.63	0.60	**0.73**	**0.82**	**0.89**	**0.93**	**0.97**	**0.99**

[a]Bold indicates the correlation is significant ($p < 0.05$). This depends on the number of degrees of freedom, calculated separately for each pair.

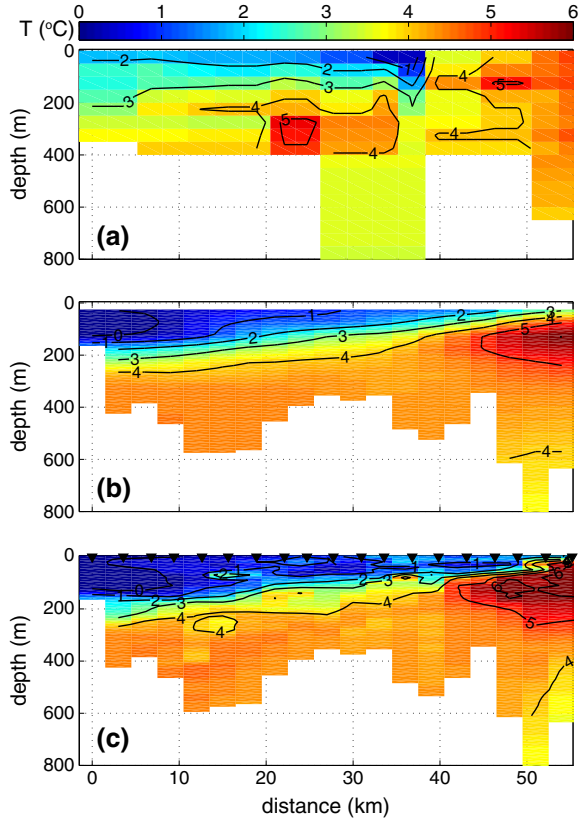

Figure 5. (a) Temperature section along the August 2004 cruise track [location in Figure 2d; *Sutherland and Pickart*, 2008] constructed from the seal temperature data. Contours are every 1 °C. (b) Temperature section along the August 2004 cruise track constructed from averaged CTD casts to match the spatial scales of the seal data averaging. (c) Original temperature section along the August 2004 cruise track from CTD casts at the stations indicated (black triangles).

same track. The seal data show a similar cold, PW wedge next to the coast with the 3 °C isotherm sloping to the seabed at a comparable depth (Figure 5). The temporal and spatial averaging used to create the seal section damped the temperature magnitudes, resulting in decreased T gradients. Despite the reduced gradients, the fact that the seal-derived section can reproduce the baroclinic EGCC point to the potential for using the seal data to investigate time variability in the transport and structure of the coastal current.

[22] The positive correlation weakens, but stays significant, down to $T_{a,200–250}$ ($R = 0.22$). Below 250 m, SST is not significantly correlated with subsurface water temperature ($R \leq 0.18$). However, $T_{a,0–50}$ is significantly correlated with temperatures down to 350 m (Table 3), suggesting that the upper 50 m contains more information on the subsurface properties than one can infer from SST alone.

[23] The seal data and correlations suggest that SST can be used as a proxy for subsurface ocean temperatures on the SE Greenland shelf, but only down to 250-m depth at most, and outside the fjords themselves. However, the AW properties presented here (Figure 4), and for other Greenland fjords elsewhere, reveal that the warmest waters are often >250 m deep [*Rignot et al.*, 2010; *Holland et al.*, 2008; *Mortensen et al.*, 2011; *Straneo et al.*, 2012]. Furthermore, mixing of AW and PW inside fjords themselves, driven by processes such as tides, internal waves, or seiches [e.g., *Mortensen et al.*, 2011; *Sutherland and Straneo*, 2012] can alter the heat content of fjord water masses or change the interface depth between AW and PW. Both of these would decrease the utility of SST as a proxy for waters reaching the glacier.

[24] One might assume that SST would be more useful as a proxy for warm mode profiles, but the seal-derived T data provide a strong caveat on that assumption. Figure 6 shows a histogram of surface layer T (calculated from the mean of the 5- and 15-m depth levels taken from the seal profiles) grouped in 0.5 °C bins and sorted by their ΔT into the warm and cold modes. The warm mode profiles do have a higher average surface layer T compared with the cold mode profiles (6.9 ± 2.0 °C to 3.8 ± 2.7 °C, respectively), but they also show that a large percentage of cold mode profiles have surface layer $T > 4$ °C, overlapping with the bulk of the warm mode profiles. This implies that one cannot assess the T structure confidently from the surface temperature alone. Overall, we find that SST data cannot be used to infer AW pathways or as a proxy for deep fjord temperatures.

[25] The mean SST data (Figure 3a) generally agree with the mean seal-based T fields ($T_{0–50}$, Figure 2) in illustrating where lateral mixing between surface layer AW and PW might occur. The highest standard deviations in $T_{0–50}$ correspond to locations of high SST gradients (Figure 3), which could hint at the location of fronts between the EGC and IC. This correlation needs to be tested more comprehensively, as the number

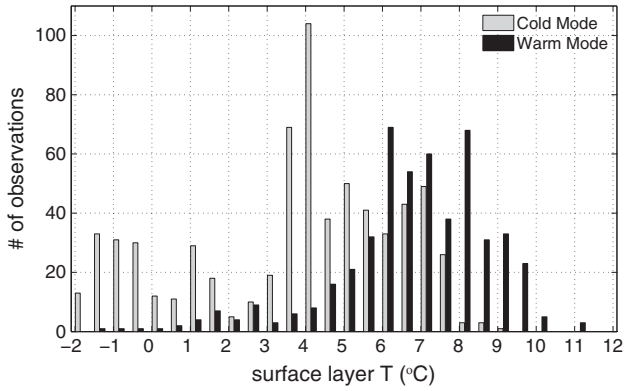

Figure 6. Histogram of surface layer temperatures from SE Greenland (mean of 5- and 15-m seal-based temperatures) grouped in 0.5 °C bins and sorted into the warm and cold modes by their ΔT.

of seal dives per bin, *N*, is not uniform, which could bias the standard deviation values. However, corresponding to the high variability regions of SST and T_{0-50} are maxima in *N* (Figure 3d), suggesting that seals preferentially dive near frontal regions that may be more biologically productive.

[26] The picture is similar in the Kangerdlugssuaq region (Figure S4), with SST qualitatively consistent with temperature fields down to 150 m (Figure S2). Deeper layers on the shelf there, however, show colder water eastward of the trough. Seal dives are concentrated near the frontal region at the shelfbreak (Figure S4). Farther south, SST fronts are again located over the small canyons cutting into the shelf (Figure S5), but no clear pattern in seal dives emerges. Note that in the KG and CF sub-regions, the standard errors were slightly higher than in the SF sub-region (Figure 3c), ranging from 0-6.3 °C for KG and 0-6.7 °C for CF (Figure S4 and S5).

4. Bathymetry

[27] The seal data also provide details on the accuracy of bathymetric products over the complex SE Greenland shelf. The bathymetric contours used in the figures presented here come from a combination of seal-derived bottom depths, new ship-derived data from inside Sermilik Fjord [*Schjøth et al*., 2012], and the one-minute gridded General Bathymetric Chart of the Oceans (GEBCO, version 20100927, http://www.gebco.net).

[28] We know that incorrect depths exist, for example, through observations at the mouth of Sermilik Fjord, where *Straneo et al*., [2010] found a channel >400 m deep, and depths >900 m in the fjord. This contrasted with the monotonic decrease in depth nearshore shown in commonly used products (Figure 7). Since seals dive to the bottom, their recorded depths can be used to examine these discrepancies. To accomplish this, we

[29] follow the general methodology developed by *Padman et al*., [2010], who used remotely sensed marine mammal dive data to update available bathymetric products around the Antarctic continental shelf.

[30] We obtained all the available bathymetric data along ship tracks in the GEODAS database [276925 points, http://www.ngdc.noaa.gov] inside the SE Greenland region. Tracklines are virtually absent near the coast (Figure 7). For all the seal dives within a 3 km radius around each trackline bathymetric data point, we calculated the percentage of the maximum dive depths by the seals that reached within 20 m of the bottom. This percentage (51%) was not sensitive to changing the search radius (to 1 km or 2 km) or excluding the harp seals. This is a greater percentage than the 30% reported for elephant seals [*Padman et al*., 2010], but is consistent with the deep diving behavior of hooded seals [*Rosing-Asvid*, 2010]. Given this percentage, we calculate the number of seal dives, $N = 4$ (this comes from the 51% calculated above), needed in the search radius to have a greater than 95% probability that the deepest dive was to the seabed. For each seal dive, if $N > 4$ within a 3 km radius, and that dive is the deepest, it is defined as the new depth.

[31] After applying this method to the Sermilik Fjord sub-region, we used a 5 km x 5 km 2-D boxcar filter to smooth the new bathymetry, as the introduction of seal-derived depths caused spikiness due to gaps in coverage. The same filter was applied to the GEBCO fields. The result (Figure 7c) shows deeper channels near many of the nearshore regions, particularly leading up to Sermilik Fjord. Differences on the order of 200-300 m were obtained near the main channel leading to Sermilik Fjord (Figure 7d,e). Updating the GEBCO depths with the newly released International Bathymetric Chart of the Oceans (IBCAO) version 3 [*Jakobsson et al*., 2012; available June 2012 at http://www.ibcao.org], did not significantly change these results. We use GEBCO as it includes IBCAO version 2.23, but extends south of 64ºN, covering the entire study region.

[32] We find significant differences for the Kangerdlugssuaq Fjord and Cape Farewell sub-regions as well (Figure S6 and S7, respectively). The trough leading to Kangerdlugssuaq Fjord has several deeper channel offshoots than observed in the original GEBCO (Figure S6). In addition, the coastal region presumably has more numerous deep channels (e.g., as near Sermilik Fjord) than shown in GEBCO, though the data at present only allows confirmation of this inside the fjord. Near Cape Farewell, the largest differences are again near the numerous embayments and canyons that line the SE Greenland continental shelf (Figure S7). More abundant trackline data here reduce the differences between GEBCO and the updated bathymetry to <100 m, which though smaller, remain significant.

5. Summary

[33] Water masses in Greenland's glacial fjords have a two-layer stratification that is a product of polar origin and Atlantic-origin waters. The interaction of these two water masses and the depth of the interface between them can substantially affect the amount of heat that fjords circulate to outlet glaciers. Here we have utilized a growing database of temperature observations collected by seals to map out summertime temperature distributions on the SE Greenland continental shelf and have examined the modes of AW properties. The seal-based data represent a new source of hydrographic data for this area with vast potential; typical ship-based or float-based (e.g., ARGO) observations are extremely scarce in space and time in the remote, fast-flowing boundary current areas characteristic of the North Atlantic subpolar gyre. This database can be easily extended to

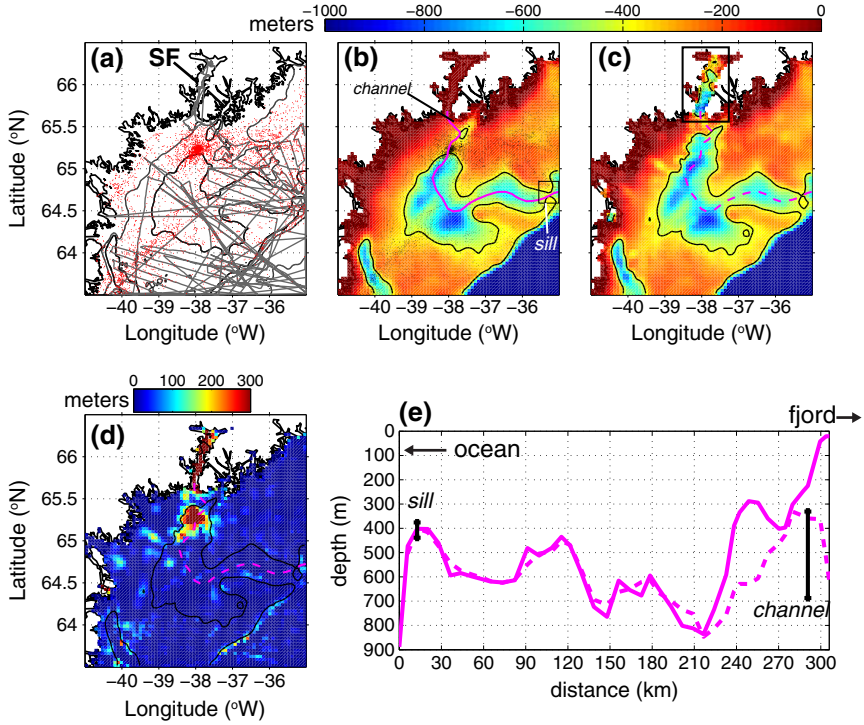

Figure 7. (a) Map showing the location of seal dives (red) and available tracklines of bathymetric data (gray) near Sermilik Fjord (SF). Original GEBCO 300- and 400-m isobaths are contoured (black). (b) Gridded GEBCO bathymetric product with seal dives (black) and the thalweg section (magenta), with the 400-m isobath (black). (c) Updated GEBCO plus seal dive depth data bathymetry, with changes inside fjord (black box) from *Schjøth et al*. [2012]. (d) Gridded differences in depth (m), where positive means updated bathymetry is deeper (note the colorbar saturates at 300 m even though differences in the fjord are >300 m). (e) Depths along the thalweg section in b (solid) and c (dashed) with depth ranges for the sill and channel areas in c.

examine other continental shelf areas off Greenland or Canada (e.g., SW Greenland, Labrador; Figure 1).

[34] Updates to available gridded bathymetric products were made with the depths derived from the deep-diving seals. The largest corrections occurred in submarine canyons that cut across the SE Greenland shelf. This application of the seal data could be applied to regions in west Greenland as well. The narrow, deep submarine canyons that funnel AW towards these glacial fjords are more widespread than ascertained from available bathymetric products, challenging future climate models that need to resolve these pathways to accurately predict ice sheet-ocean interactions.

[35] The seal-derived temperature fields showed the spatial and temporal variability in the two dominant vertical profile shapes: a warm mode with full water column AW properties, and a cold mode with the typical EGC two-layer structure of colder PW overlying the AW. The cold mode structure implies a direct advective pathway of the EGC/IC system towards the coast. The warm mode structure, on the other hand, has no polar-origin water present, implying either the passage of a warm-core IC eddy propagating towards the coast or a larger excursion of the IC past the region, so that water properties are more akin to those found in the Irminger Sea. We observed an increased percentage of the warm mode profiles near the mouth of Sermilik Fjord during the summer and fall.

[36] In addition, we found that SST cannot be used as an indicator of changes in temperature of the deepest Atlantic-origin waters that move towards these glacial fjords, although SST does correlate significantly with waters above 250 m depth. Thus, if changes in fjord properties or glacier dynamics were shown to be correlated with PW in the EGC, SST could be a viable way to assess the distribution and variability of PW on the SE Greenland shelf.

[37] **Acknowledgments.** Funding for this work came from National Science Foundation OPP grant 0909373 and OCE grant 1130008, plus the WHOI Arctic Research Initiative. The Greenland Institute of Natural Resources and the Department of Fisheries and Oceans, Canada, supported the seal tagging logistics. Bob Pickart generously allowed us use of the 2004 JR105 data. Two anonymous reviewers provided useful comments that improved the clarity and content of the manuscript.

References

Andersen, J. M, Y. W. Wiersma, G. B. Stenson, M. O. Hammill, and A. Rosing-Asvid (2009), Movement patterns of hooded seals (*Cystophora cristata*) in the Northwest Atlantic Ocean during the post-moult and pre-moult seasons, *J. Northw. Atl. Fish. Sci.*, *42*, 1–11, doi:10.2960/J.v42.m649.

Bacon, S., G. Reverdin, I. G. Rigor, and H. M. Smith (2002), A freshwater jet on the east Greenland shelf. *J. Geophys. Res.*, *107*, doi:10.1029/2001JC000935.

Boehme, L., P. L. Lovell, M. Biuw, F. Roquet, J. Nicholson, S. E. Thorpe, M. P. Meredith, M. A. Fedak (2009), Animal-borne CTD-Satellite Relay Data Loggers for real-time oceanographic data collection, *Ocean Sci.*, *5*, doi:10.5194/os-5-685-2009.

Bruce, J. G. (1995), Eddies southwest of the Denmark Strait. *Deep-Sea Res. I*, *42*, 13–29.

Dodd, P. A., K. J. Heywood, M. P. Meredith, A. C. Naveira-Garabato, A. D. Marca, and K. K. Falkner (2009), Sources and fate of freshwater

exported in the East Greenland Current, *Geophys. Res. Lett.*, *36*, L19608, doi:10.1029/2009GL039663.

Fedak, M., P. Lovell, B. McConnell, and C. Hunter (2002), Overcoming constraints of long range radio telemetry from animals: getting more useful data from smaller packages. *Integ. Comp. Biol.*, *42*, 3–10.

Freitas, C., C. Lydersen, M. A. Fedak, and K. M. Kovacs (2008), A simple new algorithm to filter marine mammal Argos locations. *Mar. Mammal Sci.*, *24*, 307–310. doi:10.1111/j.1748-7692.2007.00180.x.

Grist, J. P., S.A. Josey, L. Boehme, M. P. Meredith, F. J. M. Davidson, G. B. Stenson, and M. O. Hammill (2011), Temperature signal of high latitude Atlantic boundary currents revealed by marine mammal-borne sensor and Argo data, *Geophys. Res. Lett.*, *38*, L15601, doi:10.1029/2011GL048204.

Hammill, M. O., and G. Stenson (2000), Estimated prey consumption by harp seals (*Phoca groenlandica*), hooded seals (*Cystophora cristata*), grey seals, (*Halichoerus grypus*) and harbour seals (*Phoca vitulina*) in Atlantic Canada, *J. Northw. Atl. Fish. Sci.*, *26*, 1–23, doi:10.2960/J.v26.a1.

Hanna, E., J. Cappelan, X. Fettweis, P. Huybrechts, A. Luckman, M. H. Ribergaard (2009), Hydrologic response of the Greenland ice sheet: the role of oceanographic warming, *Hydrolog. Proc.*, *23*, doi:10.1002/hyp.7090.

Holland, D. M., R. H. Thomas, B. De Young, M. H. Ribergaard, and B. Lyberth (2008), Acceleration of Jakboshavn Isbræ triggered by warm subsurface ocean waters, *Nature Geosci.*, *1*, 659–664.

Howat, I. M., I. Joughin, and T. A. Scambos (2007), Rapid changes in ice discharge from Greenland Outlet Glaciers, *Science*, *315*, 1559–1561.

Jakobsson, M., et al. (2012), The International Bathymetric Chart of the Arctic Ocean (IBCAO) Version 3.0, *Geophys. Res. Lett.*, *39*, L12609, doi:10.1029/2012GL052219.

Jin, J., J. T. Overpeck, S. M. Griffies, A. Hu, J. L. Russell, and R. J. Stouffer, (2011), Different magnitudes of projected subsurface ocean warming around Greenland and Antarctica, *Nature Geosci.*, *4*, doi:10.1038/ngeo1189.

Kerr, G. (1984), Chords: a new temperature or sound speed profile thinning algorithm. NORDA, Mississippi, Technical Note 272.

Lydersen, C., O. A. Nost, K. M. Kovacs, and M. A. Fedak (2004), Temperature data from Norwegian and Russian waters of the northern Barents Sea collected by free-living ringed seals, *J. Mar. Sys.*, *46*, doi:10.1016/j.jmarsys.2003.11.019.

Magaldi, M. G., T. W. N. Haine, and R. S. Pickart (2011), On the nature and variability of the East Greenland Spill Jet: a case study in summer 2003, *J. Phys. Oceanogr.*, *41*, doi:10.1175/JPO-D-10-05004.1.

McFadden, E. M., I. M. Howat, I. Joughin, B. E. Smith, and Y. Ahn (2011), Changes in the dynamics of marine terminating glaciers in west Greenland (2000–2009), *J. Geophys. Res.*, *116*, F02022, doi:10.1029/2010JF001757.

Mortensen, J., K. Lennert, J. Bendtsen, and S. Rysgaard (2011), Heat sources for glacial melt in a sub-Arctic fjord (Godthåbsfjord) in contact with the Greenland IceSheet, *J. Geophys. Res.*, *116*, C01013, doi:10.1029/2010JC006528.

Murray, T., K. Scharrer, T. D. James, S. R. Dye, E. Hanna, A.D. Booth, N. Selmes, A. Luckman, A. L. C Hughes, S. Cook, P. Huybrechts (2010), Ocean-regulation hypothesis for glacier dynamics in south-east Greenland and implications for ice-sheet mass changes, *J. Geophys. Res.*, *115*, F03026, doi:10.1029/2009JF001522.

Nicholls, K. W., L. Boehme, M. Biuw, and M. A. Fedak (2008), Wintertime ocean Conditions over the southern Weddell Sea continental shelf, Antarctica, *Geophys. Res. Lett.*, *35*, L21605, doi:10.1029/2008GL035742.

Padman, L., D. P. Costa, S. T. Bulmer, M. E. Goebel, L. A. Huckstadt, A. Jenkins, B. I. McDonald, and D. R. Shoosmith (2010), Seals map bathymetry of the Antarctic continental shelf, *Geophys. Res. Lett.*, *37*, L21601, doi:10.1029/2010GL044921.

Padman, L., et al. (2012), Oceanic controls on the mass balance of Wilkins Ice Shelf, Antarctica, *J. Geophys. Res.*, doi:10.1029/2011JC007301.

Rignot, E., M. Koppes, and I. Velicogna (2010), Rapid submarine melting of the calving faces of West Greenland glaciers, *Nature Geosci.*, *3*, 187–191.

Rignot E., I. Velicogna, M.R. van den Broeke, A. Monaghan, and J. Lenaerts (2011), Acceleration of the contribution of the Greenland and Antarctic ice sheets to sea level rise, *Geophys. Res. Lett.*, *38*, L05503, doi:10.1029/2011GL046583.

Roquet, F., J.-B. Charrassin, S. Marchand, L. Boehme, M. Fedak, G. Reverdin, and C. Guinet (2011), Delayed-mode calibration of hydrographic data obtained from animal-borne satellite relay data loggers. *J. Atmos. Ocean. Tech.*, *28*, doi:10.1175/2010JTECHO801.1.

Rosing-Asvid, A. (2010), The Seals of Greenland. Ilinniusiorfik Undervisningsmiddelforlag, Nuuk, Greenland. 144 pp.

Rual, P. (1996), Onboard quality control of XBT bathy messages. Intergovernmental Oceanographic Commission of UNESCO and World Meteorological Organisation Report IOC/INF-1021: Summary of ship-of-oppportunity programmes and technical reports. Paris, 25 January 1996, 142–152.

Rudels, B., E. Fahrbach, J. Meincke, G. Budeus, and P. Eriksson (2002), The East Greenland Current and its contribution to Denmark Strait overflow. *ICES J. Mar. Sci.*, *59*, 1133–1154.

Schjøth, F., C. S. Andresen, F., Straneo, T. Murray, K. Scharrer, and A. Korablev (2012), Campaign to map the bathymetry of a major Greenland fjord. *Eos*, *Transactions*, Amer. Geophys. Union (Brief Report), *93*(14), 1.

Stearns, L. A. and G. S. Hamilton (2007), Rapid volume loss from two East Greenland outlet glaciers quantified using repeat stereo satellite imagery. *Geophys. Res. Lett.*, *34*, L05503, doi:10.1029/2006GL028982.

Straneo, F., G. S. Hamilton, D. A. Sutherland, L.A. Stearns, F. Davidson, M. O. Hammill, G. B. Stenson, and A. Rosing-Asvid (2010), Rapid circulation of warm subtropical waters in a major, *East Greenland glacial fjord, Nature Geosci.*, doi:10.1038/ngeo764.

Straneo, F., D. A. Sutherland, D. Holland, C. Gladish, G. Hamilton, H. Johnson, E. Rignot, Y. Xu, and M. Koppes (2012), Characteristics of ocean waters reaching Greenland's glaciers. *Ann. Glaciol.*, *53*(60), doi:10.3189/2012AoG60A059.

Sutherland, D. A. and R. S. Pickart (2008), The East Greenland Coastal Current: structure, variability, and forcing, *Progr. Oceanogr.*, doi:10.1016/j.pocean.2007.09.006.

Sutherland, D. A., and F. Straneo (2012), Estimating ocean heat transport and submarine melt rate in Sermilik Fjord, Greenland, using lowered ADCP profiles. *Ann. Glaciol.*, doi:10.3189/2012AoG60A050.

Vieli, A., and F. M. Nick (2011), Understanding and modeling rapid dynamic changes of tidewater outlet glaciers: issues and implications. *Surv. Geophys.*, *32*, doi:10.1007/s10712-011-9132-4.

Zwally, H. J., et al. (2011), Greenland ice sheet mass balance: distribution of increased mass loss with climate warming; 2003-07 versus 1992-2002. *J. Glac.*, *57*, 88–102.